Electronic Supplementary Material (ESI) for Journal of Materials Chemistry A.
This journal is © The Royal Society of Chemistry 2016

Electronic Supplementary Information

Ag:$BiVO_4$ dendritic Hybrid-architecture for High Energy Density Symmetric Supercapacitors

Santosh S. Patil [†],[a,b] Deepak P. Dubal[†],[c]Mohaseen S. Tamboli,[a] Jalindar Ambekar, [a]

S. S. Kolekar,[b] Pedro Gomez-Romero[c]*, Bharat B. Kale* [a] and Deepak R. Patil*

[a]Centre for Materials for Electronics Technology, Department of Electronics and Information Technology (DeitY), Govt. of India. Pune

[b]Analytical Chemistry and Material Science Laboratory, Dept. of Chem., Shivaji University, Kolhapur, India

[c]Catalan Institute of Nanoscience and Nanotechnology (ICN2), CSIC and The Barcelona Institute of Science and Technology, Campus UAB, Bellaterra, 08193 Barcelona,

Supporting information S. I. 1

Experimental:

Synthesis of Ag:$BiVO_4$ nanostructures:

Bismuth (III) nitrate [$Bi(NO_3)_3.5H_2O$], Ammonium metavanadate [NH_4VO_4] (Qualigen Chemicals Limited), Silver nitrate $AgNO_3$ (SD Fine Chemicals Limited), Ammonia NH_3 (Qualigen Chemicals Limited) and Nitric acid HNO_3 (Fisher Scientific), Ethanol C_2H_5OH (JEBSEN & JESSEN gmbH & Co. Germany) were used as starting materials. All the chemicals were of AR grade and were used without any further purification.

$BiVO_4$, Ag:$BiVO_4$ nanostructures were synthesized by facile solvothermal method. In a typical procedure, initially a mixed solvent was prepared using 5 ml HNO_3, 5 ml C_2H_5OH and 65 ml H_2O. Subsequently, 2.5 mmol of Bi $(NO_3)_3.5H_2O$ and 2.5 mmol of NH_4VO_4 were dissolved separately in each of 35 ml of as prepared solvent. The two solutions were mixed at room temperature under vigorous magnetic stirring and maintained at pH=7 by addition of NH_3. Furthermore, the solution of Ag (1 wt. %) was added dropwise and stirred for 10 min. After being cooled to room temperature naturally, the precipitate was collected and washed with distilled water and ethanol thoroughly, dried at 60^oC for 4 h and used for further characterization. For comparison pure $BiVO_4$ was also prepared were prepared by same method except use of C_2H_5OH in solvent system.

Materials Characterization:

The phase analysis of the samples were performed by X-ray diffraction (XRD) on a Rigaku-Ultima III with CuKα radiation (λ = 1.5418 Å). The surface morphology of as-prepared samples were investigated using the field-emission scanning electron microscopy (FEI Quanta

650F Environmental SEM) attached with an energy-dispersive X-ray spectroscopy (EDS) analyzer to measure the sample composition. Microstructure investigation was conducted using field emission transmission electron microscopy with a JEOL JSM 2200 FS microscope operating at 200 kV.

Electrochemical measurements

In order to check the electrochemical performances, the working electrodeswere prepared by using Doctor Blade method. For this, 85 % of active material (Ag:$BiVO_4$) was mixed with 10 % PVDF as binder and 5 % acetylene black. A few drops of N-Methyl-2-pyrrolidone (NMP, solvent) were added and the mixture was homogenized using a mortar to get a uniform paste. Finally, the paste was applied on commercial flexible carbon cloth which was further used as SCs electrodes. The resultant thin films were then annealed at 180 ^{o}C for two hours in order to remove the binder. The typical mass loading of the electrode material was around 0.5-0.9 mg/cm2. The electrochemical properties were measured using standard three electrode system which contain working electrodes ($BiVO_4$ and Ag:$BiVO_4$), counter electrode (platinum) and reference electrode (Ag/AgCl) in 6 M KOH electrolyte. Symmetric cell was constructed in a 3-way Teflon Swagelok cell using two identical electrodes of Ag:$BiVO_4$ with polypropylene separator sandwiched between them and few drops of 6 M KOH electrolyte. Two channels from potentiostat were connected together in such a way that one channel records voltage between two electrodes (positive and negative) and other channel records potential contributed from positive and negative electrodes with respect to reference electrode. All electrochemical measurements (cyclic voltammetry (CV) and galvanostatic charge-discharge techniques) were carried out using a Biologic VMP3 potentiostat.

Supporting information S. I. 2

Reaction and growth mechanism for Ag:$BiVO_4$ nano-architecture formation

The evolution of well-defined dendrite morphology via hydrothermal route invites the discussion for reaction mechanism and formation mechanism in detail. The plausible reactions taking place in the Ag:$BiVO_4$ hybrid architecture are shown below,

$$Bi(NO_3)_3.5H_2O + HNO_3 + H_2O \rightarrow BiONO_3 + 3\,HNO_3 \quad \ldots\ldots. (1)$$

$$Ag + NH_3 \rightarrow Ag(NH_3)_2^+ \quad \ldots\ldots. (2)$$

$$NH_4VO_3 + BiONO_3 + Ag(NH_3)_2^+ + H_2O \rightarrow Ag{:}BiVO_4 + NH_3 + HNO_3 \quad \ldots\ldots. (3)$$

In a present chemical reaction, the bismuth cations and vanadium anions are provided by the hydration of $BiNO_3.5H_2O$ and NH_4VO_3, respectively. Initially, the hydrolysis of $Bi(NO_3)_3.5H_2O$ takes place and form a soluble $BiONO_3$ which readily react with VO_3^- ions at Ph ~ 6-7 forming pale yellow precipitate of tetragonal $BiVO_4$. During hydrothermal treatment, after getting sufficient thermal energy, the generated $BiVO_4$ nuclei aggregates and converted to highly crystalline form of monoclinic $BiVO_4$ crystals. Meanwhile, the addition of Ag into the reaction medium produces $Ag(NH_3)_2^+$ complex on reaction with NH_3.[1] The formed $Ag(NH_3)_2^+$ complex ions takes sufficient thermal energy to drive-reach the surface of $BiVO_4$ sites wherein gets reduced to Ag by ethanol under high temperature and pressure conditions.[1,2] It is expected that simultaneous nucleation of $BiVO_4$ and Ag might occur which further grow according to self assembly and Ostwald ripening mechanism. It is known that a higher monomer (precursor) concentration in solution generally favors 1D growth whereas the lower monomer concentration favors 3D growth.[3] In the present case, the hydrothermal reaction system with relatively lower reactant concentration, sufficient temperature (180 ^oC) and optimum pH (= 7)

value provides higher chemical potential, and faster ion movement, thereby resulting in formation Ag:$BiVO_4$ hybrid dendritic structures. It is noteworthy that the proper growth of dendrites was observed for Ag:$BiVO_4$ compared to pure $BiVO_4$ sample which might be due to effect of addition of C_2H_5OH as a reducing agent in solvent system, playing a key role on facilitating crystal growth and tailoring the morphology.

From morphology evolution point of view, initially, primary particles starts to aggregate to minimize surface energy, offering driving force for self assembly. The self assembly proceeds by the rotation of particles via Brownian motion and short-range interaction between the particles, causing formation of smaller branches (rod like) that act as building blocks for dendrites. Furthermore, due to prolonged reaction time (24 h) the continuous growth of larger particles are occurred at expense of smaller particles known as Ostwald ripening to form larger subunits or branches to adjust it to achieve a minimum total surface free energy.[3] It is presumed that the an isotropic growth of formed branches along [001] direction is responsible for formation of 3D hierarchical $BiVO_4$ dendritic structures.[4] Thereby, the obtained Ag:$BiVO_4$ dendritic structures preserves several key features of interlinked connectivity through branched surfaces, propound effect of Ag nanocrystals, improved surface properties and stability. Therefore it really sense to examine the performance of this kind of material for energy application.

Supporting information S. I. 3

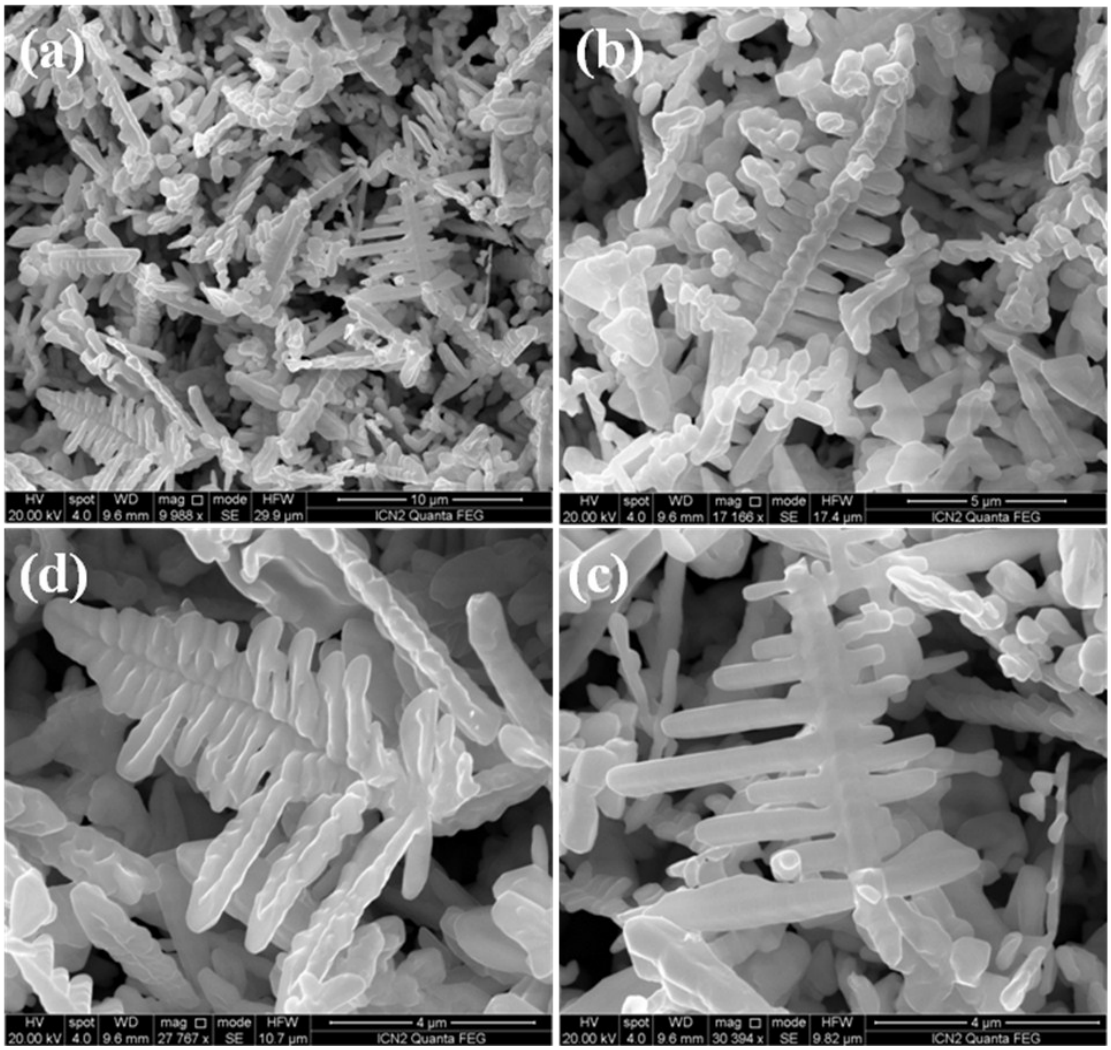

Fig. S.I. 3 FESEM images of Ag:$BiVO_4$ with different magnifications

Supporting information S. I. 4

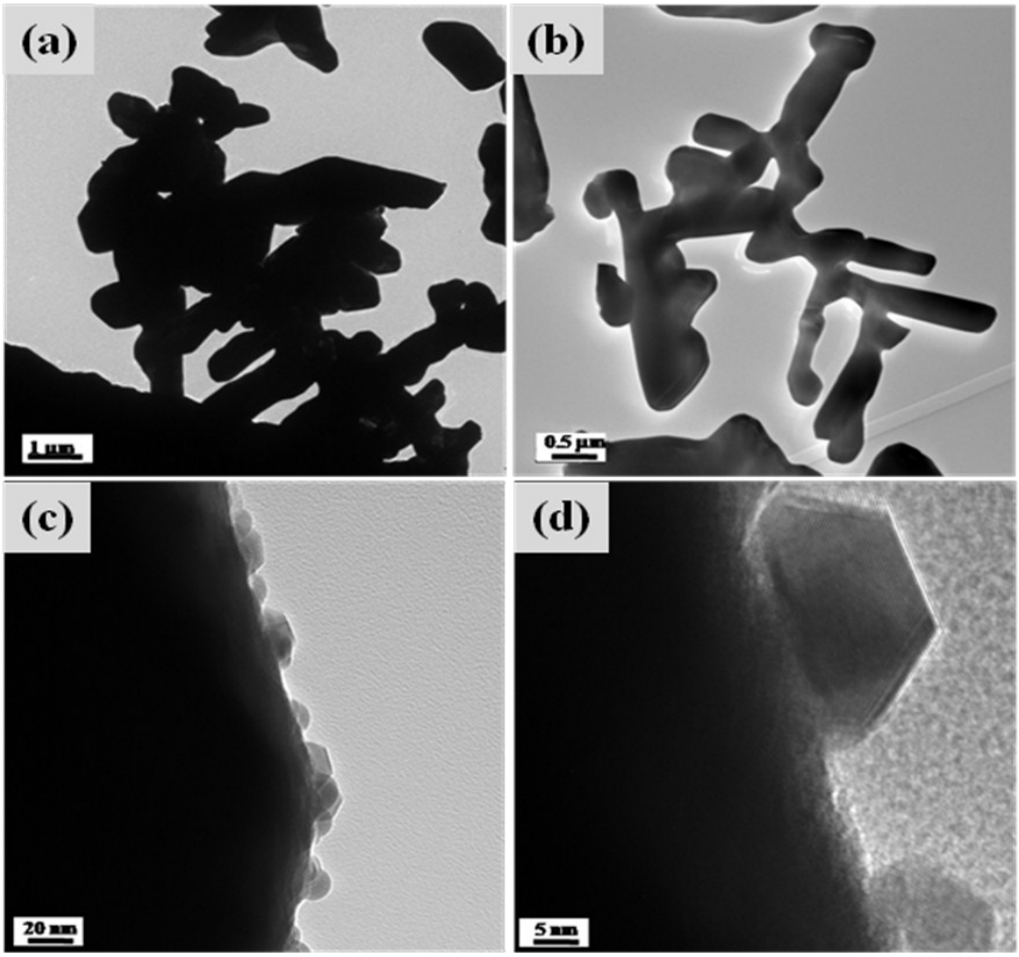

Fig. S.I. 4 FETEM images of Ag:$BiVO_4$ with different magnification

Supporting information S.I. 5

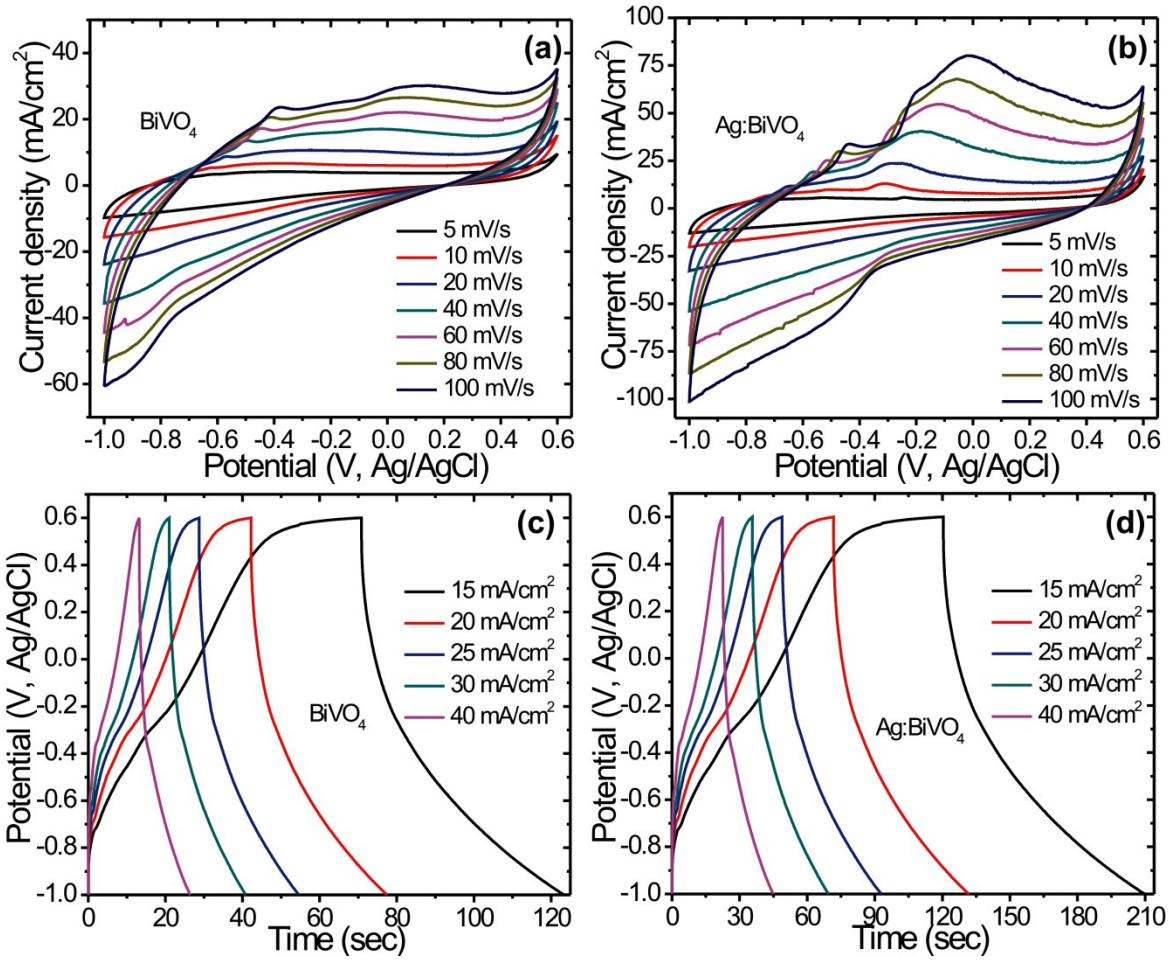

Fig. S. I. 5 Cyclic voltammetry (CV) curves of (a) $BiVO_4$ and (b) Ag:$BiVO_4$ electrodes at different scanning rates and Galvanostatic charge/discharge (CD) curves of (c) $BiVO_4$ and (d) Ag:$BiVO_4$ microstructures at different current densities.

Supporting information S.I. 6

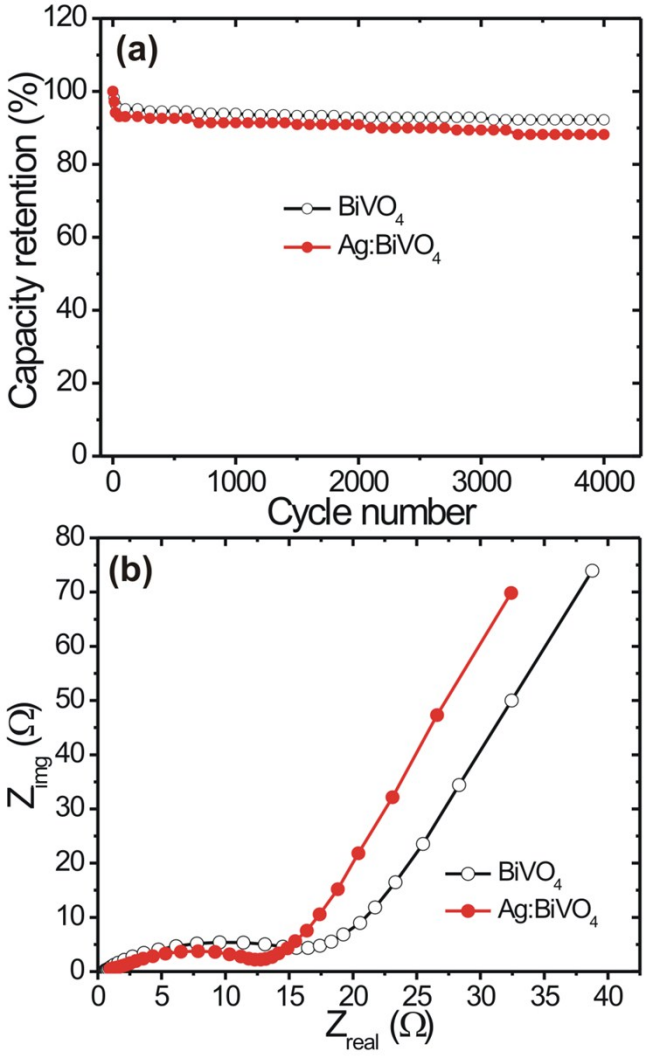

Fig. S.I. 6 Cyclic performance of $BiVO_4$ and $Ag:BiVO_4$ electrodes (b) Nyquist plots of $BiVO_4$ and $Ag:BiVO_4$ electrodes (inset shows the equivalent circuit diagram of Nyquist plots)

Fig. S.I.6 (a) depicts the cycle performance of $BiVO_4$ and $Ag\text{-}BiVO_4$ electrodes which showing excellent cycling stability with around 92 % capacity retention after 4000 cycles. The impedance spectra were recorded in order to investigate the bulk solution resistance (R_e), charge transfer resistance (R_{ct}), and Warburg resistance (Z_w) of as synthesized electrode materials. Fig. S.I.6 (b)

displays the Nyquist plots of impedance spectra of the $BiVO_4$ and Ag-$BiVO_4$ with inset showing the equivalent circuit diagram of Nyquist plots. Both the plots showed similar behavior in terms of curve shape (semicircle) except change in the resistance value. The obtained semi circles are due to charge transfer resistance (R_{ct}) which represents how fast the charge transfer takes place at electrode-electrolyte interface. The comparatively lower value of charge transfer resistance (R_{ct}) indicates the improved charge transfer in Ag:$BiVO_4$ hybrid architecture. Further, the small (R_e) value reveals good electrical conductivity of Ag:$BiVO_4$ compared to pristine $BiVO_4$ electrode. This proves that the synergetic effect between Ag and $BiVO_4$ hybrid plays a key role for improving the electrochemical properties by facilitating electronic conduction as well as charge discharge processes. All these results directly reveal the feasibility of using Ag:$BiVO_4$ as a negative electrode for high performance supercapacitor device.

Supporting information S.I. 7

The cell (device) capacitance (C) and volumetric capacitance of the symmetric devices were calculated from their CVs according to the following equation:

$$C_{cell} = \frac{Q}{\Delta V} \quad \text{.....(1)}$$

$$C_A = \frac{Q}{A\,x\,\Delta V} \quad \text{..... (2)}$$

where, C_A and C_V are areal and volumetric capacitances, respectively. *Q*(C) is the average charge during the charging and discharging process, V is the volume (cm^3) of the whole device (The area and thickness of our symmetric cells is about 0.785cm^2(Area, $A=\pi r^2$, $3.14\times(0.5)^2$) and 0.088 cm. Hence, the whole volume of device is about 0.069 cm^3, *ΔV* (V) is the voltage window. It is worth mentioning that the volumetric capacitances were calculated taking into account the volume of the device stack. This includes the active material, the flexible substrate and the separator with electrolyte.

Alternatively, the cell capacitance (C_{cell}), areal (C_A) and volumetric (C_V) capacitance of the electrode (C_V) was estimated from the slope of the discharge curve using the following equations:

$$C_{cell} = \frac{Ix\Delta t}{\Delta V} \quad \text{..... (3)}$$

$$C_A = \frac{Ix\Delta t}{A\,x\,\Delta V} \quad \text{and} \quad Cv = \frac{Ix\Delta t}{V\,x\,\Delta V} \quad \text{..... (4)}$$

Where *I* is the applied current, V is the volume (cm^3) of the whole device (the whole volume of our device is about 0.069 cm3), Δt is the discharging time, ΔV (V) is the voltage window. Volumetric energy (E, Wh/cm3) and power density (P, W/cm) of the devices were obtained from the following equations:

$$E = \frac{1}{2\ x\ 3600} C_V \Delta V^2$$

$$P = \frac{3600\ xE}{\Delta t}$$

where*E* (Wh/cm^3*)* is the energy density, *CV* is the volumetric capacitance obtained from Equation (5) and ΔV (V) is the voltage window, P (W/cm3) is the power density.

Supporting information S.I. 8

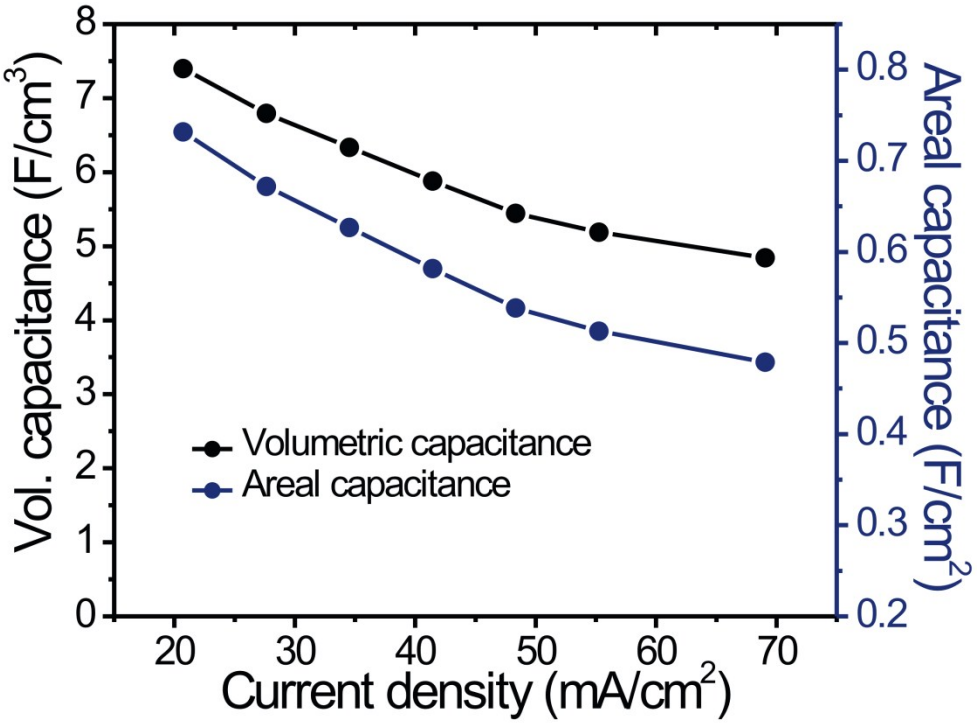

Fig. S.I. 8 Variation of Volumetric capacitance and Areal capacitance with current density of Ag:$BiVO_4$/Ag:$BiVO_4$ symmetric supercapacitors

Table S1: Electrochemical properties of Ag:$BiVO_4$/Ag:$BiVO_4$ symmetric supercapacitors in 6 M KOH electrolyte

Current density (A/g)	Discharge time (sec)	Capacitance		Specific energy	
		Volumetric (F/cm^3)	Gravimetric (F/g)	Volumetric (mWh/cm^3)	Gravimetric (Wh/kg)
3.1	56.5	7.39	108.1	2.63	38.43
4.1	38.92	6.79	99.2	2.41	35.30
5.1	29.04	6.33	92.6	2.25	32.92
6.1	22.46	5.88	85.9	2.09	30.55
7.1	17.82	5.44	79.5	1.93	28.285

Table S2: Comparison of Supercapacitor values of Transition Metal Oxide (TMOs) based electrodes

Electrode	Device	Electrolyte	Volumetric capacitance	Max. Vol. Energy Density at power density	Reference
Ag:$BiVO_4$	Symmetric	6M KOH	7.39 F/cm^3	2.63 mWh cm^{-3} at 0.558 W cm^{-3}	Present work
H-TiO_2 @MnO_2 //H-TiO_2@C	Asymmetric	5 M LiCl	0.68 F/cm^3	0.30 mWh cm^{-3} at 0.23 W cm^{-3}	5
Co_9S_8//Co_3O_4 @RuO_2	Asymmetric	3M KOH	3.42 F/cm^3	1.21 mWh cm^{-3} at 13.29 W cm^{-3}	6
VO_x//VN	Asymmetric	5M LiCl electrolyte	1.35 F/cm^3	0.61 mWh cm^{-3} at 0.85 W cm^{-3}	7
MoS_2	Asymmetric	0.5 M Na_2SO_4	-	0.016 Wh cm^{-3} at 0.62 W cm^{-3}	8
laser-scribed graphene(LSG) //LSG	Symmetric	1.0 M H_3PO_4	0.42 F/cm^3	0.09 mWh cm^{-3}at 0.1 W cm^{-3}	9

References:

1. S. S. Warule, N. S. Choudhari, R. T. Khare, J. D. Ambekar Kale, B. B. Kale and M. A. More, *CrystEngComm.*, 2013, **15**, 7475.
2. Y. Zheng, L. Zheng, Y. Zhan, X. Lin, Q. Zheng and K. Wei, *Inorg. Chem.* 2007, **46**, 6980.
3. R. P. Panmand, R. H. Patil, B. B. Kale, L. K. Nikam, M. V. Kulkarni, D. K. Thombre, W. N. Gade and S. W. Gosavi, *RSC Adv.,* 2014, **4**, 4586.
4. L. Zhou, W. Wang and H. Xu, Cryst. *Growth Des.*, 2008, **8**, 728.
5. X. Lu, M. Yu, G. Wang, T. Zhai, S. Xie , Y. Ling, Y. Tong, and Y. Li, *Adv. Mater.* 2013, **25**, 267.
6. J. Xu, Q. Wang, X Wang, Q. Xiang, B. Liang, D. Chen and G. Shen, *ACS Nano*, 2013 **7**, 5453.
7. X. Lu, M. Yu, T. Zhai, G. Wang, S. Xie, T. Liu, C. Liang, Y. Tong and Y. Li, *Nano Lett.* 2013, **13**, 2628.
8. M. Acerce, D. Voiry and M. Chhowalla, *Nat. Nanotech.*, 2015, **10**, 313.
9. M. F. El-Kady, , V. Strong, , S.Dubin and R. B. Kaner, *Science*, 2012, **335**, 1326.